ELSEVIER

Journal of Chromatography B, 736 (1999) 153–166

JOURNAL OF CHROMATOGRAPHY B

www.elsevier.com/locate/chromb

Aggregation of recombinant hepatitis B surface antigen induced in vitro by oxidative stress

Dina Tleugabulova[a,*], Viviana Falcón[b], Eduardo Pentón[c], Minerva Sewer[d], Yosvany Fleitas[e]

[a]*Quality Control Department, National Center for Bioproducts, P.O. Box 6048, Havana 6, Cuba*
[b]*Department of Physical Chemistry, Center for Genetic Engineering and Biotechnology, P.O. Box 6162, Havana, Cuba*
[c]*Vaccine division, Center for Genetic Engineering and Biotechnology, P.O. Box 6162, Havana, Cuba*
[d]*Development Department, National Center for Bioproducts, P.O. Box 6048, Havana 6, Cuba*
[e]*Production Plant, National Center for Bioproducts, P.O. Box 6048, Havana 6, Cuba*

Received 11 May 1999; received in revised form 30 August 1999; accepted 5 October 1999

Abstract

In order to examine whether oxygen radicals could be responsible for aggregation of recombinant hepatitis B surface antigen (HBsAg) during its assembly in yeast, purified HBsAg was oxidized with ammonium peroxodisulphate (AP) and analyzed by non-denaturing and denaturing size exclusion chromatography, immunoassay and immunoelectron microscopy. As a result, peroxodisulphate radicals induced a reproducible aggregation of HBsAg. At 44 m*M* AP, the aggregation process took a few hours and the resulting structures were large, branched and non-antigenic. During more gentle oxidation with 9 m*M* AP and 20–80 μ*M* Cu^{2+}, a continuous structural modification to HBsAg delaying for tens of hours preceded the aggregation event. During this pre-aggregation period, peroxidation of HBsAg lipids and covalent cross-linking of S protein chains occurred that led a complete loss of antigenicity of oxidized particles. In contrast, yeast-derived HBsAg aggregate is decomposed to S monomers under reducing conditions and recognized by anti-HBsAg polyclonal and monoclonal antibodies, suggesting that is has been assembled in vivo from antigenic and reversibly cross-linked particles. Based on these observations, we conclude that oxidation, at least with respect to the specific molecular sites oxidized by AP, is not a primary event in HBsAg aggregate formation in vivo. Since oxidized HBsAg was shown to be irreversibly cross-linked and non-antigenic, there are no suitable techniques for detection HBsAg oxidation in biological samples. Hence, at present, the magnitude of the in-vivo oxidative damage to HBsAg cannot be evaluated and thus, whether the plasma-derived HBsAg undergoes radical-induced oxidation in the course of viral hepatitis remains to be established. If this occurs, this process is expected to contribute to low HBsAg levels in chronic hepatitis B carriers, failure of the currently available immunoassays to identify HBsAg-positive blood donors and inconsistency in the results provided by HBsAg- and anti-HBsAg-based tests in several recent reports.

Keywords: Hepatitis B surface antigen; Viral proteins

*Corresponding author. Fax: +53-7-338439.

0378-4347/99/$ – see front matter
PII: S0378-4347(99)00453-3

1. Introduction

Recombinant hepatitis B surface antigen (HBsAg) produced in *Pichia pastoris* is self-assembled intracellularly into 22-nm lipoprotein particles ($M_r \sim 2.5 \times 10^6$) composed by approximately 100 units of a non-glycosylated S protein (M_r 24000) and yeast lipids [1,2]. Formation of the HBsAg particle is a complex process requiring the coordinated synthesis and assembly of S protein, triglycerides, free cholesterol, esterified cholesterol, free fatty acids and phospholipids [3,4]. It is presently accepted that this process involves (1) S protein mRNA transcription and translation, (2) translocation of S protein across the endoplasmic reticulum membrane and formation of S protein dimers, (3) transport of transmembrane dimers to a post-endoplasmic reticulum pre-Golgi compartment where the luminal HBsAg particle is assembled [5–7].

There are many difficulties in handling this unusually complex multi-protein assembly in analytical studies. Half of the S monomer of HBsAg consists of a continuous stretch of hydrophobic residues (Pro, Trp, Phe, Leu and Ile) that form three hydrophobic domains, two of which likely span the lipid bilayer of the assembled particle [6]. S protein also contains 14 Cys residues, which participate in an extensive disulfide cross-linking within the assembled particle. After the removal of HBsAg-associated lipids, the strongly hydrophobic S protein chains are immediately precipitated from aqueous solutions [8] and, as a consequence of this, are not easily separated by reversed-phase HPLC (RP-HPLC) elution systems containing significant amounts of water. Previously published methodology for separation of hydrophobic proteins includes RP-HPLC methods applying alcoholic organic modifiers [9,10] and formic acid as the ion-pairing reagent [11], as well as normal-phase techniques [12]. However, we were unable to obtain consistent results with these methods. S protein binds irreversibly to the commonly used column packing with chain lengths of the alkyl substituents of either four, eight or 18 carbon atoms utilizing standard acetonitrile–TFA gradients (data not shown). Additionally, its recovery is not satisfactory even if the pore size of the RP-HPLC sorbents is extended to 30 nm [13]. S protein is not easily separated by hydrophobic interaction chromatography, judging from the appearance of numerous broad peaks and correspondingly low intensity and resolution [13]. Whole HBsAg particles also bind irreversibly to the RP-HPLC supports [13], probably due to their lipid-associated structure. As most lipid-containing proteins [14], HBsAg is likely to be efficiently delipidated by alkyl-silica surfaces followed by on-column precipitation of the cross-linked S protein chains.

Another problem for the structural characterization of HBsAg is its resistance to trypsin cleavage. Whole HBsAg particles are not cleaved by trypsin at enzyme to protein ratios from 1:50 to 1:14, whereas the reductive treatment of HBsAg generates a unique trypsin cleavage site at Lys122 [15]. Even following HBsAg reduction and aminoethylation of Cys residues, only a few soluble peptides are released. Due to these problems, only 25% of S primary structure had been established using trypsin digestion [15]. Later, an additional 60% of the previously unobserved sequence regions were assessed by chymotryptic digestion of the reduced and carboxymethylated S protein chains followed by peptide mapping by fast atom bombardment mass spectrometry [16].

In size exclusion chromatography (SEC), HBsAg produces one broad peak corresponding to co-elution of several structurally heterogeneous forms of HBsAg, such as low-order multi-particle aggregates with a variable extent of aggregation, correctly assembled particles and particles with partially degraded S chains [17]. However, SEC is capable of separating larger multi-particle aggregates composed of more than ten particles in an individual peak with lower retention time [18]. As shown by electron microscopy, this peak corresponds to HBsAg species with an almost continuous spectrum of the degrees of aggregation [17]. Such size heterogeneity of SEC-separated HBsAg aggregates, in turn, limits the usefulness of modern on-line detection systems, e.g. low-angle laser light scattering [19–22], viscosimetry [23,24] and photon correlation spectroscopy [25,26], for investigating key size properties and the composition of the aggregated material. The lack of protein standards with molar masses $>10^6$ [27] impedes even a relative estimation of M_r range for aggregated HBsAg.

Our interest in HBsAg aggregation was spurred by a finding that a large portion of yeast-derived HBsAg

(about 40%) is irreversibly aggregated in the crude material [18]. Apparently, the ultrastructure of HBsAg particles is preserved after aggregation [18], indicating that folding of HBsAg precedes aggregation and therefore, this latter process does not compete with productive folding which is important for biological activity of yeast-derived HBsAg. Hence, by preventing or limiting this aggregation, it would be possible to improve the recovery of recombinant product. On the other hand, aggregation of recombinant HBsAg in yeast may occur by a similar pathway that the aggregation of its natural homologue in hepatocytes and plasma of chronic hepatitis B carriers [28–30]. At present, the detailed biochemical properties of HBsAg and its aggregates in hepatocytes are still largely unknown and clear-cut evidence for their biological functions during hepatitis B infection is missing. It cannot be excluded that HBsAg aggregation plays a role in the immunopathogenesis of hepatitis B virus. The relevance of this unexplored subject stimulated us to perform experiments on the molecular characterization of HBsAg aggregates, but without successful results. The aggregate-containing solution displays a characteristic opalescence indicating a limited solubility of HBsAg aggregates in aqueous solutions. This opalescence is preserved in 8 *M* urea and diminished after treatment with 5% SDS. After reduction and carboxymethylation of HBsAg aggregate, the reduced material requires at least 0.5% SDS to remain soluble. After the removal of SDS, S protein forms a precipitate soluble exclusively in pure TFA [unpublished results]. When the reduced and carboxymethylated sample is digested by chymotrypsin in the presence of 0.5–1% SDS and the detergent further removed by the ion-exchange precolumn, a large portion of the digested material is unrecoverable from the RP-HPLC matrix. Perhaps, some useful structural information may be obtained from amino acid analysis and several additional experiments that are currently in progress.

In the absence of suitable analytical strategies, SEC seems to be the only method capable of detecting aggregate formation in the HBsAg-containing solutions. Since SEC shows a limited potential to resolve components with comparable M_r exhibiting only relatively small structural changes, the only purpose of using this method in the present study was to detect the formation of HBsAg aggregates after subjection of the purified protein to different stress conditions.

Recently provided evidence for the occurrence of radical-mediated processes in the *yeast S. cerevisiae* [31,32] led us to postulate that HBsAg aggregation in yeast is induced by oxygen radicals. Although there is a set of cell defense systems to mitigate the damaging effects of oxygen radicals [33], injury cannot be excluded. Radical-mediated modifications in DNA, RNA, proteins and cell membrane are well-documented in superior organisms during aging [34], apoptosis [35], neurodegenerative diseases [36] and iron metabolism imbalance [37]. Additionally, HBsAg is a potential target for oxygen radicals due to its particle structure [38] and a high content of labile amino acid residues (Cys, Trp, Tyr, Met) and phospholipids [39,40]. The particles of mineral and biological origin, such as silica [41], carbide [42], asbestos [43], melanin [44,45] and β-amyloid [46] were shown to be critical sites for appearance of free radical activity. In a similar manner, yeast-derived HBsAg particles may provide key loci for the formation of oxygen radicals.

If it is true that HBsAg aggregation is caused by oxidation, then this process should be mimicked in-vitro by incubation of purified HBsAg with reactive oxygen species. To test this, the effect of different radical-generating agents on the aggregation state of HBsAg was analyzed by SEC. Metal-catalyzed oxidation, being more gentle and site-specific [47], was used to evaluate whether a catalyst alone is capable of inducing aggregation. Potentially, HBsAg may also contain traces of lipid peroxidation products capable of initiating oxidation and aggregation of HBsAg in the presence of Cu^{2+} ions. In order to evaluate whether the presence of exogenous oxygen radicals is necessary for aggregation, ammonium peroxodisulphate (AP) was chosen. This reagent is commonly used to induce polyacrylamide gel polymerization. Decomposition of AP in aqueous solutions leads to liberation of peroxodisulphate oxygen radicals that not only efficiently affect the structure of proteins by preponderant modification of sulphydryl groups and oxidation of tyrosine and tryptophan residues [48–50], but also initialize their polymerization. This last aspect might have important implications for HBsAg aggregation.

2. Experimental

2.1. Materials

All the reagents mentioned in the text were of analytical grade and obtained from Merck (Darmstadt, Germany). The reagents used in electron microscopy were from Agar Scientific (Essex, UK). All solutions were made in Milli-Q grade water. Phosphate-buffered saline (PBS) contained 1.7 m*M* KH_2PO_4, 7.9 m*M* Na_2HPO_4, 2.7 m*M* KCl and 250 m*M* NaCl, pH 7.0. Recombinant HBsAg, cloned and expressed in yeast *Pichia pastoris*, was purified by a multistep procedure [51] and provided as a solution in PBS from the National Center for Bioproducts (Havana, Cuba). This solution was filtered through a 0.22-μm filter (Millipak 200, Millipore, Bedford, MA, USA) and stored at 4°C until use (up to 6 months). An anti-HBsAg mouse monoclonal antibody and an anti-HBsAg polyclonal lamb polyclonal antibody used for the immunodetection of HBsAg were provided from the Center for Genetic Engineering and Biotechnology (Havana, Cuba).

2.2. Oxidation of HBsAg

To promote formation of HBsAg aggregates during oxidation, incubations were done with a high concentration of HBsAg (1.25 mg/ml). Oxidation was induced by AP (9, 22, 44 m*M*), Cu^{2+} (20– 100 μ*M*), Fe^{2+} (50, 100 μ*M*), H_2O_2 (100, 500 m*M*) or by mixtures of them (Table 1). The homogenized solution (PBS; final volume, 520 μl) was incubated at 37°C for the time periods indicated in table. The oxidation was stopped by addition of 2% (w/v) NaN_3 (final concentration, 0.1%, w/v) and the degree of HBsAg modification was estimated by ELISA and SEC.

Table 1
SEC study of HBsAg aggregation under different oxidizing conditions[a]

Oxidation conditions	Incubation time (h)	Aggregation result
50 μ*M* Cu^{2+}	100	−
100 μ*M* Cu^{2+}	100	−
50 μ*M* Fe^{2+}	100	−
100 μ*M* Fe^{2+}	100	−
100 m*M* H_2O_2	100	−
500 m*M* H_2O_2	100	−
100 m*M* H_2O_2+100 μ*M* Cu^{2+}	100	−
500 m*M* H_2O_2+100 μ*M* Cu^{2+}	100	−
100 m*M* H_2O_2+100 μ*M* Cu^{2+} + 100 μ*M* Fe^{2+}	100	−
9 m*M* AP	100	−
15 m*M* AP	35	+
22 m*M* AP	8	+
44 m*M* AP	2	+
44 m*M* AP+44 m*M* TEMED	80	−
9 m*M* AP+50 μ*M* Cu^{2+}	60	+
9 m*M* AP+80 μ*M* Cu^{2+}	60	+
9 m*M* AP+100 μ*M* Cu^{2+}	50	+
44 m*M* AP+20 μ*M* Cu^{2+}	2	+
44 m*M* AP+50 μ*M* Cu^{2+}	1	Precipitation
44 m*M* AP+50 μ*M* Cu^{2+}+44 m*M* TEMED	80	−

[a] Conditions of analysis: TSK G5000 PW (600×7.5 mm I.D.) supplied with a TSK GPW guard column (75×7.5 mm I.D.); eluent, 0.05% NaN_3; flow-rate, 0.5 ml/min; detection, 280 nm; injection volume, 100 μl, HBsAg, 1.25 mg/ml (PBS). For detailed experimental conditions see Section 2. TEMED, *N,N,N′,N′*-tetramethylethylenediamine. Aggregation result (+) corresponds to 100% conversion of HBsAg into its aggregated form.

2.3. Analysis of oxidized HBsAg

The degree of aggregation was monitored by SEC using a 2248 pump (Pharmacia-LKB, Uppsala, Sweden), a Knauer degasser (Berlin, Germany), a Pharmacia 2141 variable-wavelength UV detector operated at 280 nm and a Pharmacia 2221 programmable integrator. The system was fitted with a TSK G5000 PW column (Tosohaas; 600×7.5 mm I.D., 17 μm) and a TSK GPW guard column (75×7.5 mm I.D.), both obtained from Tosohaas, Stuttgart, Germany. The samples (20 μl) were injected by means of a 200-μl loop and eluted with PBS at 0.5 ml/min. An aqueous solution containing sodium azide (0.05%, m/v) as a singlet oxygen quencher was used as the mobile phase.

The degree of protein cross-linking was monitored by denaturing SEC. Oxidized HBsAg samples (100 μl) were reduced with 417 m*M* dithiothreitol, 4.2% (w/v) sodium dodecyl sulfate (SDS) and 16% (v/v) 2-mercaptoethanol (20 μl) for 10 min at 100°C, as previously described [52]. Aliquots of the reduced samples (30 μl) were injected onto a TSK G4000 SW column (600×7.5 mm I.D., 13 μm, Tosohaas, Stuttgart, Germany), eluted with 0.1 *M* Tris–HCl in 0.3% SDS, pH 8.0 at 0.6 ml/min and detection performed at 280 nm.

2.4. Measurement of conjugated dienes

The HBsAg (1.25 mg/ml, PBS), incubated with 9 m*M* AP and 50 μ*M* Cu^{2+} at 37°C, was continuously monitored at 234 nm to detect the degree of structural alteration of HBsAg. The experiments were performed in duplicate using three different HBsAg preparations. The results were given as mean absorbance values, setting the absorbance of native HBsAg as zero [53].

2.5. Binding of oxidized HBsAg to an anti-HBsAg polyclonal antibody

The HBsAg samples oxidized for different periods (0–20 h) with 9 m*M* AP and varying Cu^{2+} concentrations were applied to polystyrene micro-titration plates (F96 Maxisorb Nunc-Immuno Plate, Nunc, Denmark) previously coated with an anti-HBsAg lamb polyclonal antibody. Binding of oxidized HBsAg was detected via an anti-HBsAg-horseradish peroxidase conjugate (Center for Genetic Engineering and Biotechnology, Havana, Cuba). The working standard preparation of HBsAg was calibrated against an international standard obtained from the Paul Erlich Institute (Frankfurt, Germany). The experiments were performed in duplicate using three different HBsAg preparations tested. The results were given as mean percentages, setting the antibody-binding of native HBsAg to 100%. The latter was incubated at 37°C for the same time period as the oxidized sample.

2.6. Binding of oxidized HBsAg to an anti-HBsAg monoclonal antibody

The HBsAg samples oxidized for different periods (0–20 h) with 9 m*M* AP and varying Cu^{2+} concentrations were directly applied to polystyrene micro-titration plates at the amounts ranging from 4 to 0.06 μg per well. Detection was with a biotinylated anti-HBsAg monoclonal antibody prepared using the Biotinylation Kit according to the manufacturer's instructions (Sigma, St. Louis, MO, USA). Bound biotinylated antibody was revealed by addition of streptavidin–peroxidase conjugate (Sigma, St. Louis, MO, USA). The experiments were performed in duplicate using three different HBsAg preparations. The results were given as mean percentages, setting the antibody-binding of native HBsAg to 100%. The latter was incubated at 37°C for the same time period as the oxidized sample.

2.7. Transmission electron microscopy

Two drops of HBsAg solution (0.1 mg/ml) in PBS (1.7 m*M* KH_2PO_4, 7.9 m*M* Na_2HPO_4, 2.7 m*M* KCl and 250 m*M* NaCl, pH 7.0) were placed for 5 min onto a 400-mesh copper grid coated with formvar carbon film and excessive sample removed. Grids were stained with uranyl acetate and examined in a Jeol-JEM 2000EX transmission electron microscope (Tokyo, Japan) with an acceleration voltage of 80 kV and 40 000-fold image magnification.

2.8. Immunoelectron microscopy

The grids coated with HBsAg samples were floated with six drops of 1% BSA in PBS before transfer to a drop of the PBS-diluted (dilution, 1:20) anti-HBsAg monoclonal antibody for incubation at room temperature (30 min). After washing in 'gold buffer' (0.5 *M* Tris–Cl, pH 7.0, 0.15% NaCl, 0.5 mg/ml polyethylene glycol 20 000, 0.1% NaN_3) to remove unbound antibody molecules, the grids were floated with two drops of 'gold buffer'-diluted (dilution, 1:200) protein A-gold complexes (particle diameter, 15 nm; Center for Genetic Engineering and Biotechnology, Havana, Cuba) for 30 min at room temperature. Finally, the grids were subsequently washed with six drops of 'gold buffer' and two drops of distilled water. After draining and staining with 1% phosphotungstic acid, the grids were examined as described.

3. Results and discussion

3.1. Aggregation of oxidized HBsAg

In SEC, purified HBsAg gives a broad peak at 33 min (Fig. 1A), whereas its supramolecular aggregates migrate at 23.2 min [18]. Hence, the appearance of a sharp peak at 23.2 min in the chromatogram of oxidized HBsAg would indicate aggregate formation.

Table 1 summarizes the effect of different oxidants on the aggregation state of HBsAg in PBS. Incubation of HBsAg with Cu^{2+} ions did not induce aggregation, but affected the recovery of the HBsAg peak (Fig. 1B). The same result was observed after incubations of HBsAg with Fe^{2+} ions and H_2O_2 (data not shown). In each case, recovery was gradually improved by decreasing the ionic strength of the mobile phase and HBsAg was completely recovered when 0.05% (w/v) NaN_3 was used as the eluent system. The obvious recovery loss could reflect increased interactions of modified HBsAg with the column matrix, presumably attributable to electrostatic forces [54], which are eliminated by lowering the ionic strength of the medium. After incubation of HBsAg with Cu^{2+} ions, there was also a marked negative shift in retention time of the peak maximum from 33 to 30 min (Fig. 1A and B), eventually attributable to slight modifications during oxidative treatment than to recovery problems. The absence of a peak attributable to aggregated HBsAg indicated that Cu^{2+}, Fe^{2+} and H_2O_2 did not effect in-vitro conversion of native protein into its aggregated form. Perhaps, HBsAg requires specific modification before aggregation starts. The effective size of a protein is increased at lower ionic strengths, due to reduction in electrostatic shielding [55]. This explains a negative shift (about 3.5 min) in retention

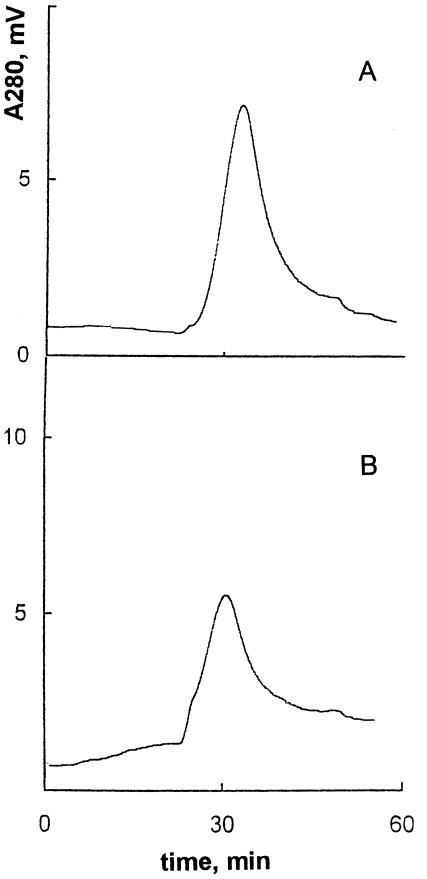

Fig. 1. SEC chromatogram of native HBsAg prior (A) and after oxidation with 100 μ*M* Cu^{2+}. Conditions: TSK G5000 PW (600×7.5 mm I.D.) supplied with a TSK GPW guard column (75×7.5 mm I.D.); eluent, PBS, pH, 7.0; flow-rate, 0.5 ml/min; detection, 280 nm; injection volume, 100 μl; HBsAg, 1.25 mg/ml; retention time, 33.01 min (A), 30.11 min (B). Oxidation conditions: Cu^{2+}, 100 μ*M*; PBS, pH 7.0, 37°C, incubation for 24 h.

time of the peak maximum of native HBsAg when 0.05% NaN_3, instead of PBS, was used for elution (data not shown).

Ammonium peroxodisulphate (AP), added at the concentration of 44 m*M*, rapidly converted HBsAg into enormously large and branched structures (Fig. 2A). These structures resembled long filaments which are commonly observed in plasma and hepatocytes of hepatitis B-infected persons [28–30]. In SEC, the incubation of HBsAg with AP led to a continuous conversion of HBsAg peak into the 23.2 min-peak, corresponding to its aggregates (Fig. 3). The aggregation process was prevented by addition of *N*,*N*,*N′*,*N′*-tetramethylethylendiamine (TEMED) from the beginning of the experiment (Table 1). This reagent seems to exert a quenching effect on aggregation, which, perhaps, may be effected via scavenging of free oxygen radicals produced by AP decomposition. It is worthy to mention that the concentration of HBsAg had no influence on the onset of aggregation (data not shown) and it appears that it was mainly caused by the absolute concentration of the oxidizing agent and not by the concentration ratio between oxidant and HBsAg.

The aggregation process was slowed down by using lower AP concentrations (Table 1). At 9 m*M* AP, the presence of a catalyst was necessary because neither Cu^{2+} ions nor AP alone were able to initiate aggregation. Under these more gentle conditions, the aggregation velocity was essentially lowered (Table 2). There was a long pre-aggregation period of 22–30 h during which the SEC profile of HBsAg was

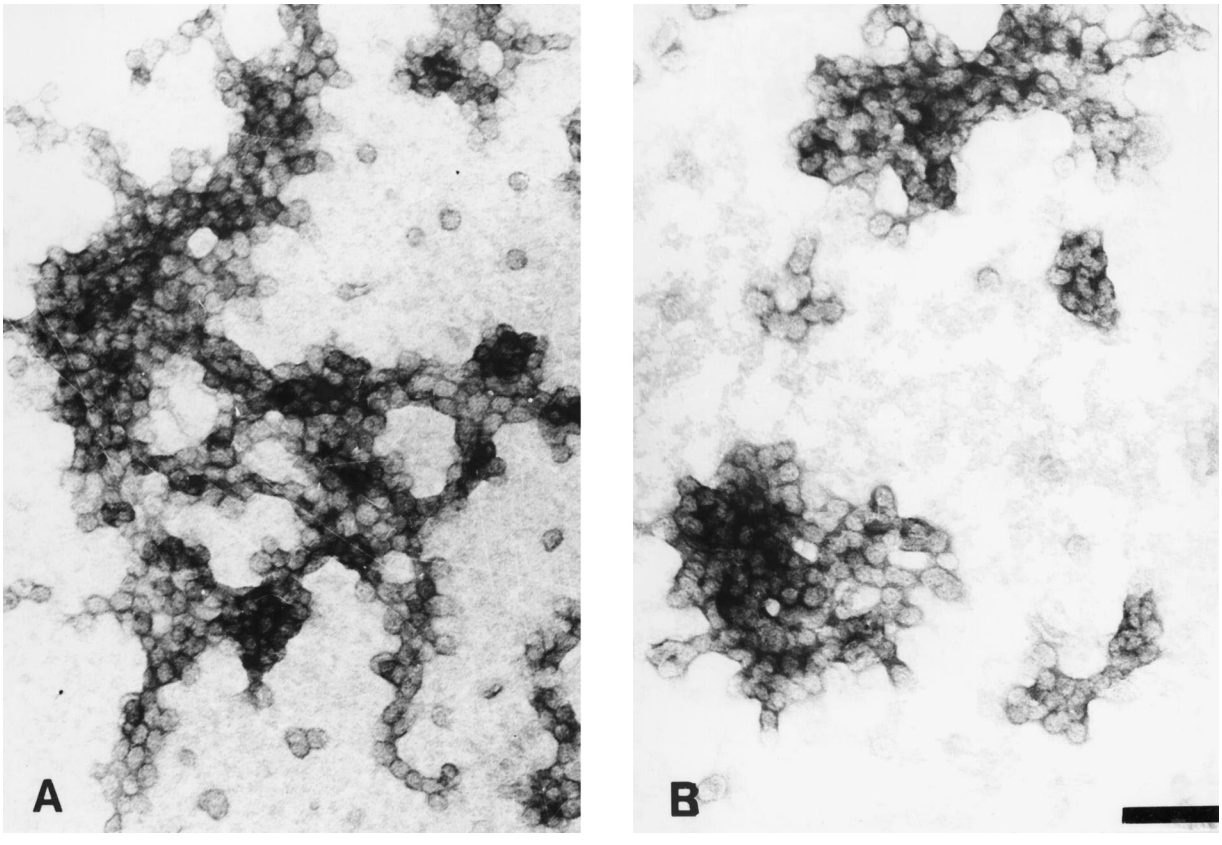

Fig. 2. Transmission electron micrographs of HBsAg oxidized with 44 m*M* AP (A) and 9 m*M* AP/100 μ*M* Cu^{2+} (B); for detailed experimental conditions see Section 2; magnification factor, 40 000; scale bar, 100 nm.

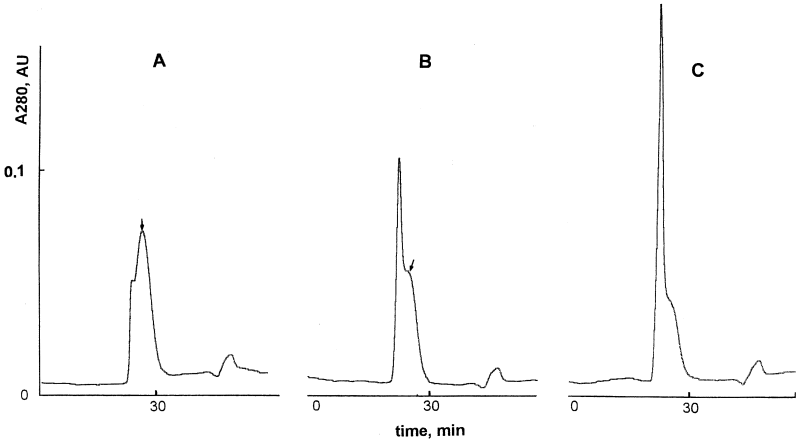

Fig. 3. Changes in the SEC profile of HBsAg during AP-induced oxidation. Conditions: TSK G5000 PW (600×7.5 mm I.D.) supplied with a TSK GPW guard column (75×7.5 mm I.D.); eluent, 0.05% NaN_3; flow-rate, 0.5 ml/min; detection, 280 nm; injection volume, 100 μl; HBsAg: 1.25 mg/ml; oxidation conditions: AP, 44 m*M*; PBS, pH, 7.0, 37°C, incubation for 5 min (A), 1 h (B) and 2 h (C). Arrows indicate the HBsAg peak; retention time, 26.75 min.

essentially unchanged (data not shown). Once initiated, the aggregation process was completed after 25–40 h of oxidation, depending on the initial Cu^{2+} concentration. Resulting HBsAg aggregates were smaller (Fig. 2B) and closer in size and shape to the yeast-derived aggregate [18].

3.2. Peroxidation of HBsAg lipids

By decreasing the velocity of HBsAg aggregation, it was possible to detect multiple oxidative modifications to HBsAg occurring during the pre-aggregation period. It was found that the pH of the HBsAg

Table 2
The pH values and aggregate content at different stages of HBsAg oxidation[a]

Incubation time, (h)	20 μ*M* Cu^{2+}		50 μ*M* Cu^{2+}		80 μ*M* Cu^{2+}	
	pH	Aggregation, %	pH	Aggregation, %	pH	Aggregation, %
0	7.0	–	7.0	–	7.0	–
6	6.8	–	6.5	–	6.2	–
22	6.2	–	5.0	–	4.5	–
30	5.8	–	4.5	10.8	3.8	18.5
45	5.3	22.6	4.0	33.3	3.3	90.6
60	4.5	50.7	3.5	68.7	3.3	100.0
70	4.0	59.0	3.5	100.0	3.0	100.0
90	3.6	100.0	3.0	Precipitation	2.8	Precipitation
0	8.5	–	8.5	–	8.5	–
6	8.0	–	8.0	–	7.0	–
22	7.5	–	7.5	11.0	6.5	–
30	7.0	–	6.3	22.3	5.8	21.8
45	6.5	18.9	5.8	39.4	5.2	94.5
60	6.0	55.1	5.5	70.5	4.8	100.0
70	5.8	61.2	5.3	100.0	4.5	100.0
90	5.0	100.0	4.8	Precipitation	4.0	Precipitation

[a] Chromatographic conditions as in Table 1. Oxidation conditions: Cu^{2+}, 20, 50 and 80 μ*M*; AP, 9 m*M*; HBsAg, 1.25 mg/ml (PBS); incubation at 37°C.

solution, initially adjusted to 7.0, began to decrease almost immediately after addition of AP and Cu^{2+}. In most cases, aggregation occurred when the pH of the solution reached the isoelectric point of HBsAg (Table 2), which is 4.6 (unpublished results). However, at an initial pH 8.5, aggregation was shown to occur independently whether or not the pH of the solution reached the isoelectric point of HBsAg. At these latter conditions aggregation was pH-independent and starts at the same oxidation periods in all the experiments performed (Table 2). After aggregation, further pH-decrease led to precipitation of HBsAg (Table 2).

Since the initial solution contained the purified HBsAg only, the observed pH-decrease can be interpreted as a consequence of the HBsAg-related modifications. Accordingly, there was an almost immediate increase in the absorbance at 234 nm (Fig. 4), due to formation of conjugated dienes, indicating peroxidation of HBsAg lipids [53]. This increase was maximal after 1 h of oxidation and then slightly decreased. However, when oxidation was extended to more than 2 h, a further increase in the absorbance values presumably attributable to formation of lipid peroxides was observed. In general, lipid hydroperoxides are unstable and further decomposed to aldehydes [55]. These latter are rapidly oxidized to acids in aqueous solutions, explaining thus the observed pH-decrease in the course of HBsAg oxidation (Table 2). Aldehydes can also modify HBsAg lipids and protein in a close proximity to them [56,57], leading to a continuous release of lipid and protein peroxides observed in Fig. 4. Initially, such modifications do not produce changes in HBsAg size and thus are undetectable by SEC.

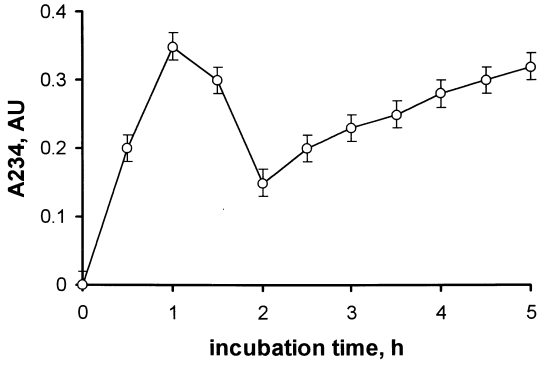

Fig. 4. Mean conjugated diene formation measured as the difference in absorbance at 234 nm following oxidation of HBsAg with 9 m*M* AP/50 μ*M* Cu^{2+}. For detailed experimental conditions see Section 2. Values are means±standard deviations.

3.3. Antigenic reactivity of oxidized HBsAg

During the pre-aggregation period, oxidized HBsAg completely lost recognition by an anti-HBsAg polyclonal and monoclonal antibodies. As shown in Fig. 5 and 6, this loss was accelerated at higher initial pH and Cu^{2+} concentrations. In immunoelectron microscopy, the loss of antigenicity was corroborated for the extensively oxidized HBsAg, but not for the gently oxidized, aggregated HBsAg (Fig. 7), where this latter was immunostained with the anti-HBsAg monoclonal antibody, despite the completely lacking immunoreactivity in a normal immunoassay (data not shown). The antibody molecules recognize multiple repetitive epitopes in the native HBsAg, and even if one of these epitopes is preserved after oxidation, it will be identified by immunogold staining. The oxidized HBsAg was stained with the formation of hoops around gold particles (Fig. 7B) that is typical for native HBsAg [58]. However, single and disperse HBsAg molecules were presumably recognized, rather than whole aggregated structures, suggesting that original epi-

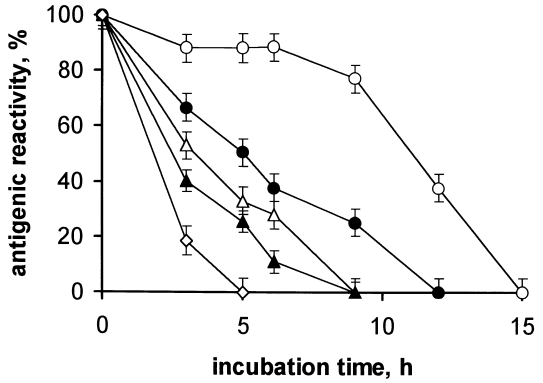

Fig. 5. Binding of oxidized HBsAg to anti-HBsAg polyclonal antibody in a solid-phase immunoassay. For detailed experimental conditions see Section 2. Oxidation conditions: HBsAg, 1.25 mg/ml; AP, 9 m*M*; Cu^{2+}, 0 μ*M* (open circles and rhombs), 20 μ*M* (filled circles), 50 μ*M* (open triangles), 80 μ*M* (filled triangles); pH, 7.0, 8.5 (open rhombs); incubation, 37°C. Values are means±standard deviations.

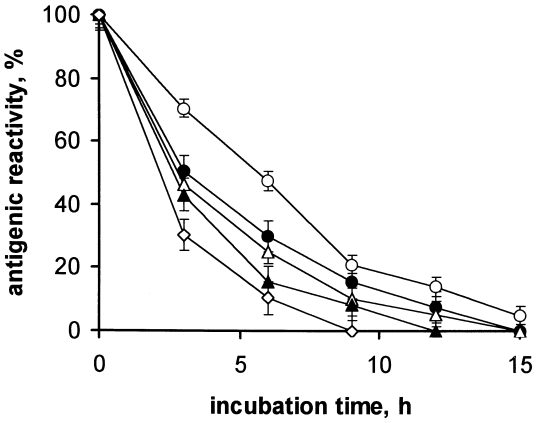

Fig. 6. Binding of oxidized HBsAg to anti-HBsAg monoclonal antibody in a solid-phase immunoassay. For detailed experimental conditions see Section 2. Oxidation conditions: HBsAg, 1.25 mg/ml; AP, 9 m*M*; Cu^{2+}, 0 μ*M* (open circles and rhombs), 20 μ*M* (filled circles), 50 μ*M* (open triangles), 80 μ*M* (filled triangles); pH, 7.0, 8.5 (open rhombs); incubation, 37°C. Values are means±standard deviations.

topes are preserved in few HBsAg molecules within the aggregate. In conlusion, although oxidation affects the antigenic sites on HBsAg, several original epitopes may be preserved under gently oxidizing conditions.

3.4. Covalent cross-linking of S protein chains in the oxidized HBsAg assessed by denaturing SEC

Linkage of HBsAg particles within the aggregate structure may occur by different molecular mechanisms, such as hydrophobic interactions, hydrogen bonding, covalent cross-linking of S protein chains via free thiol groups or another modified amino acid residues. However, the fact that aggregated HBsAg does not dissociate to single particles at a high ionic strength or after its treatment with detergents (data not shown) indicates that the covalent cross-linking between aggregated particles should be a primary mechanism of aggregation. Similarly to native HBsAg, the yeast-derived aggregate is efficiently disrupted to S monomers after heating with SDS and thiol agents, suggesting that the sites of aggregation are essentially the same as those for reduction. In order to verify whether the HBsAg aggregates produced in vitro by oxidation with AP are also disrupted to S monomers under reducing conditions, HBsAg samples were oxidized with AP and Cu^{2+} ions, then reduced and subjected to denaturing SEC.

In denaturing SEC, the reduced sample is directly loaded on to the TSK G4000 PW column equilibrated with the SDS-containing buffer. Native HBsAg is commonly reduced by thiol agents to S protein dimers, monomers and degradation products [17] which are unsatisfactorily resolved on the TSK G4000 PW column: S monomers elute in the peak maximum, whereas S dimers and degradation products elute in the forward and backward shoulders, respectively (Fig. 8A). However, all these reduced species are well-separated from the non-reduced HBsAg, which elutes in the exclusion volume of the TSK G4000 PW column (Fig. 9).

As shown in Fig. 8B and C, oxidized HBsAg was not disrupted to S monomers after reduction with 2-mercaptoethanol and DTT: Instead of the S monomer-peak, a peak attributable to non-reduced aggregates appeared in the chromatogram. When this peak was collected and the eluate repeatedly reduced, no recoverable S monomers were detected in denaturing SEC and SDS-electrophoresis (data not shown), indicating that polymerization of S monomers had been occurred. Hence, in the oxidized HBsAg, the sites of oxidation are not the same as those for reduction. Since the corresponding aggregate is non-antigenic, insoluble in the absence of SDS and does not migrate in SDS-polyacrylamide gel (data not shown), no structural assignment can be done, at least by conventional methods. Probably, the AP-induced oxidative cross-linking of S chains involves the modified Tyr or Trp residues on the particle surface. The peak corresponding to elution of degradation products was recovered after the oxidative treatment of HBsAg, suggesting that the degraded protein chains do not participate in the oxidative cross-linking.

We previously demonstrated that during oxidation of HBsAg with low concentrations of AP and Cu^{2+} ions, there was a large time period prior aggregation. It is worth mentioning that the cross-linking of S monomers was detected during this pre-aggregation period, when the oxidized HBsAg was still kept free from aggregation (Table 2). We can speculate that under gentle oxidation, the oxidative cross-linking initially involves S chains of the same particle. Both protein cross-linking (Fig. 8) and peroxidation of

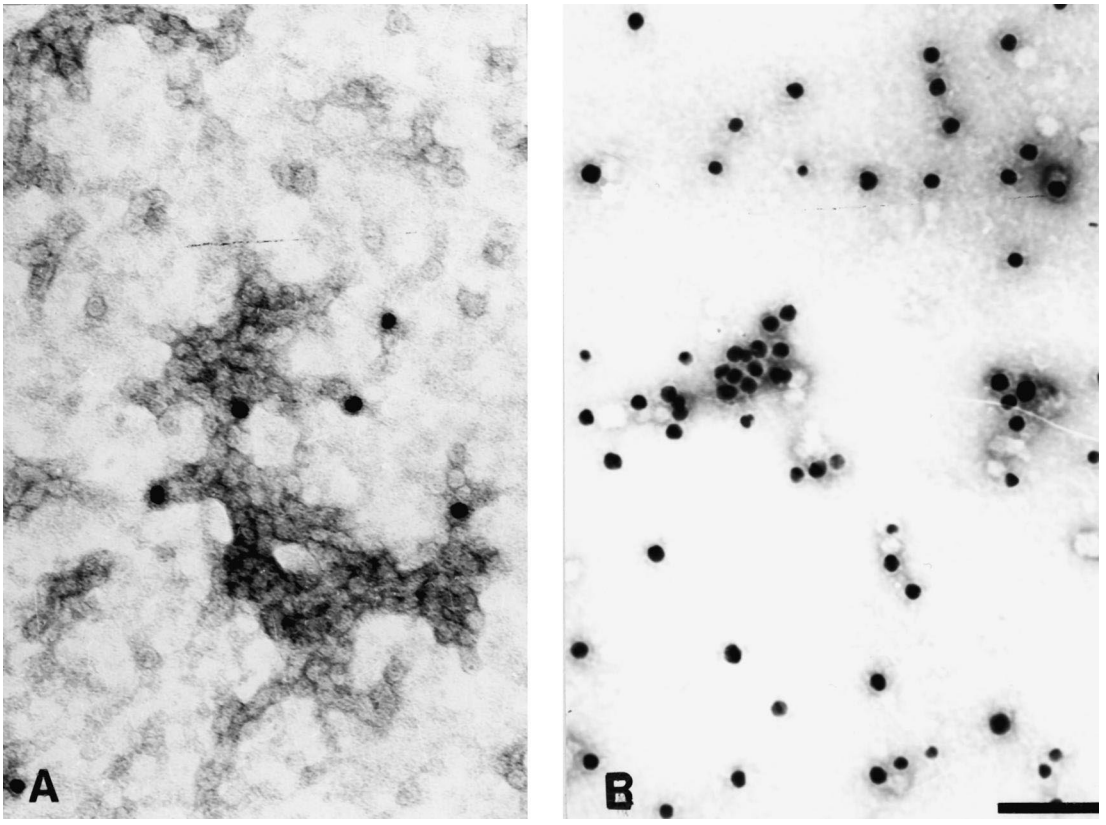

Fig. 7. Immunoelectron microscopy of HBsAg oxidized with 44 m*M* AP (A) and 9 m*M* AP/100 μ*M* Cu^{2+} (B); for detailed experimental conditions see Section 2; magnification factor, 40 000; scale bar, 100 nm.

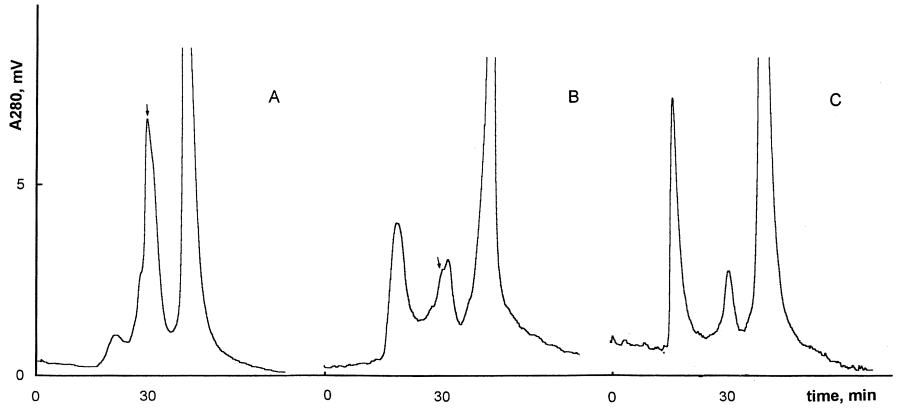

Fig. 8. SEC profiles of native (A) and oxidized (B,C) HBsAg after reduction with thiol reagents. Conditions of analysis: TSK G4000 SW (600×7.5 mm I.D.); eluent, 0.1 *M* Tris–HCl, 0.3% SDS, pH 8.0; flow-rate, 0.6 ml/min; detection, 280 nm; HBsAg: 1.25 mg/ml; injection volume, 25 μl; reducing buffer, 417 m*M* DTT, 4.2% (w/v) SDS and 16% (v/v) 2-mercaptoethanol. Oxidation conditions as in Fig. 5; incubation at 37°C for 30 min (B) and 1 h (C). Arrows indicate the reduced S protein monomer-peak; retention time, 29.81 min.

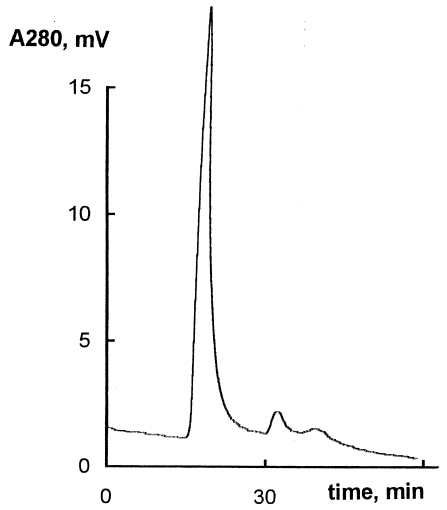

Fig. 9. SEC-profile of native HBsAg treated with 4.2% SDS for 10 min at 100°C. Conditions of analysis as in Fig. 8. HBsAg, 1.8 mg/ml; injection volume, 75 μl; retention time of non-reduced HBsAg, 16.11 min.

HBsAg lipids (Fig. 4) were initiated during the pre-aggregation period, indicating that these processes are closely related. It is likely that HBsAg lipids are oxidized to peroxides and these latter products further contribute to the cross-linking of S protein chains. Although these processes cause modifications in the HBsAg structure, as judged from the complete loss of its recognition by anti-HBsAg antibodies (Fig. 5,6), they seem to have minor implications for M_r of HBsAg and thus remain undetectable by SEC. Only after a larger extent of HBsAg modification, aggregation of oxidized HBsAg particles is detected.

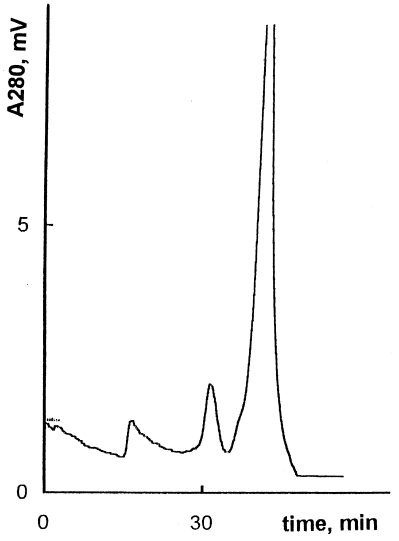

Fig. 10. SEC profile of oxidized and aggregated HBsAg after its reduction with thiol reagents. Conditions of analysis and oxidation as in Fig. 7. HBsAg, 1.25 mg/ml; injection volume, 25 μl; oxidation at 37°C for 60 h.

In denaturing SEC, the aggregation event was accompanied by a drastic loss in the intensity of the cross-linked HBsAg-peak (Fig. 10). Accordingly, the recovery of the injected protein was also considerably affected data not shown), suggesting that the observed loss in the peak intensity was due to precipitation of the aggregated protein on to the column matrix.

4. Conclusions

Incubation of HBsAg particles with peroxodisulphate radicals leads to a reproducible formation of supramolecular aggregates whose ultrastructure is similar to that of the yeast-derived aggregates. At low AP concentrations, peroxidation of HBsAg lipids, irreversible cross-linking of S protein monomers and biological inactivation of HBsAg molecules precedes the aggregation event. In contrast, yeast-derived HBsAg aggregate is presumably composed by disulfide cross-linked monomers [17] and well-recognized by anti-HBsAg polyclonal and monoclonal antibodies [18], suggesting that is has been assembled in vivo from antigenic and reversibly cross-linked particles. Based on these observations, we conclude that oxidation, at least with respect to the specific molecular sites susceptible to oxidation by AP, is not a primary event in HBsAg aggregate formation in vivo.

Since peroxodisulphate radicals converts HBsAg into the irreversibly cross-linked and non-antigenic protein, HBsAg oxidation, if it occurs in yeast, will escape detection by all the currently available HBsAg-screening tests, e.g. radioimmunoassay, western blot and RP-HPLC. In the absence of suitable techniques, the magnitude of the in-vivo oxidative damage to HBsAg cannot be evaluated.

The fact that oxidized proteins are commonly cross-linked and biologically inactive is neither

particularly novel nor surprising. Nevertheless, it was important to demonstrate this experimentally for HBsAg, because a possible radical damage to HBsAg in living cells has never been considered before. Oxidative stress and lipid peroxidation in humans after the onset of viral hepatitis and liver cancer is well-documented in more than 150 reports published since 1978 [59]. When subjected to oxygen radicals and products derived from lipid peroxidation, HBsAg can undergo oxidation. This phenomenon, if occurs, could be responsible in part for low HBsAg levels in chronic hepatitis B carriers, failures of the currently available immunoassays to identify HBsAg-positive donors and inconsistencies in the results provided by HBsAg- and anti-HBsAg- based tests [60]. Since none of the immunoassays based on recognition of native HBsAg will efficiently detect its oxidized form, alternative methods should be developed for detection of oxidized HBsAg in biological samples.

References

[1] J. Marcelo, M.Sc. Thesis, Havana, Center for Genetic Engineering and Biotechnology, 1999.
[2] E. Pentón, V. Muzio, M. Gonzalez-Griego, Biotecnología aplicada 11 (1994) 1.
[3] F. Gavilanes, J.M. Gonzalez-Ros, D. Peterson, J. Biol. Chem. 257 (1982) 7770.
[4] F. Gavilanes, J. Gomez-Gutierrez, M. Aracil, J.M. Gonzalez-Ros, J.A. Ferragut, E. Guerrero, D. Peterson, Biochem. J. 265 (1990) 857.
[5] V. Muzio, E. Pentón, in: G. Padrón (Ed.), Bases Moleculares Para El Estudio de Las Hepatitis Virales, Elfos, 1998, p. 119.
[6] V. Bruss, E. Gerhardt, K. Vieluf, G. Wunderlich, Intervirology 39 (1996) 23.
[7] A.J. Huovila, A.M. Eder, S.D. Fuller, J. Cell Biol. 118 (1992) 1305.
[8] H. Mehdi, X. Yang, M.E. Peeples, Virology 217 (1996) 58.
[9] G.E. Tarr, J.W. Crabb, Anal. Biochem. 131 (1983) 99.
[10] G. Allmaier, B.H. Chao, H.G. Khorana, K. Biemann, The determination of the location and nature of amino acid substitutions in biosynthetic bacteriorhodopsin, in: Proceeding of the 34th Annual Conference on Mass Spectrometry and Allied Topics, American Society for Mass Spectrometry, Cincinnati, OH, 1986, p. 308.
[11] R. Bollhagen, M. Schmiedberger, E. Grell, J. Chromatogr. A 711 (1995) 181.
[12] K.L. Lerro, R. Orlando, H. Zhang, P.N. Usherwood, K. Nakanishi, Anal. Biochem. 215 (1993) 38.
[13] D.O. O′Keefe, A.M. Paiva, Anal. Biochem. 230 (1995) 48.
[14] W.C. Wimley, S.H. White, Anal. Biochem. 213 (1993) 213.
[15] D.L. Peterson, N. Nath, F. Gavilanes, J. Biol. Chem. 257 (1982) 10414.
[16] M.E. Hemling, S.A. Carr, C. Capiau, J. Petre, Biochemistry 27 (1988) 699.
[17] D. Tleugabulova, V. Falcón, E. Pentón, J. Chromatogr. A (1999) in press.
[18] D. Tleugabulova, V. Falcón, M. Sewer, E. Pentón, J. Chromatogr. B 716 (1998) 209.
[19] I.S. Krull, H.H. Stuting, S. Kryzsko, J. Chromatogr. 442 (1988) 29.
[20] R. Mhatre, H.H. Stuting, I.S. Krull, J. Chromatogr. 502 (1990) 21.
[21] R. Mhatre, I.S. Krull, J. Chromatogr. 591 (1992) 139.
[22] R. Mhatre, I.S. Krull, Anal. Chem. 65 (1993) 283.
[23] I.S. Krull, R. Mhatre, J. Cuniff, LC·GC Magazine 13 (1995) 30.
[24] R.L. Qian, R. Mhatre, I.S. Krull, J. Chromatogr. A 787 (1997) 101.
[25] M.E. Szulc, R. Mhatre, J. Mazzeo, I.S. Krull, in: B.L. Karger, W. Hancock (Eds.), Methods in Enzymology Series, Academic Press, 1996, p. 175.
[26] M.E. Szulc, I.S. Krull, in: L. Snyder, J. Glajch, J.J. Kirkland (Eds.), Practical HPLC Method Development, Wiley- Interscience Publishers, New York, 1997, p. 111.
[27] W.K.R. Barnikol, H. Potzschke, J. Chromatogr. A 685 (1994) 221.
[28] P. Roingeard, C. Sureau, Hepatology 28 (1998) 1128.
[29] B. Monges, J.P. Remacle, G. Monges, H. Payan, Pathol. Biol. 29 (1981) 143.
[30] M.A. Gerber, S. Hadziyannis, C. Vissoulis, F. Schaffner, F. Paronetto, H. Popper, Am. J. Pathol. 75 (1974) 489.
[31] N.G. Howlett, S.V. Avery, Appl. Environ. Microbiol. 63 (1997) 2971.
[32] D.J. Jamieson, Redox Rep. 1 (1995) 89.
[33] P.H. Proctor, in: J. Miquel (Ed.), CRC Handbook of Free Radicals and Antioxidants in Biomedicine, Vol. 1, CRC Press, Boca Raton, 1989, p. 209.
[34] B.S. Berlett, E.R. Stadtman, J. Biol. Chem. 272 (1997) 20313.
[35] M.D. Jacobson, Trends Biochem. Sci. 21 (1996) 83.
[36] C.W. Olanow, Trends Neurol. Sci. 16 (1993) 439.
[37] M. Gerlach, D. Ben-Shachar, P. Riederer, B.H. Youdim, J. Neurochem. 63 (1994) 793.
[38] K. Donaldson, P.H. Beswick, P.S. Gilmour, Toxicol. Lett. 88 (1996) 293.
[39] S. Li, Ch. Schoneich, R. Borchardt, Biotech. Bioeng. 48 (1995) 490.
[40] D. Steinberg, J. Biol. Chem. 272 (1997) 20963.
[41] C.N. Daniel, Y. Mao, U. Saffiotti, Free Radic. Biol. Med. 14 (1993) 463.
[42] D. Lison, P. Carbonelle, L. Mollo, R. Lauwerys, B. Fubini, Chem. Res. Toxicol. 6 (1995) 600.
[43] P.P. Simeonova, M. Luster, Am. J. Resp. Cell Mol. Biol. 12 (1995) 676.
[44] G. Benzi, A. Moretti, Neurobiol. Aging 16 (1995) 661.
[45] C.C. Felix, J.S. Hyde, T. Sarna, R.C. Sealy, J. Am. Chem. Soc. 100 (1978) 3922.

[46] S.C. Bondy, S.X. Guo-Ross, A.T. Truong, Brain Res. 799 (1998) 91.
[47] C.E. Thomas, S.D. Aust, in: J. Miguel (Ed.), CRC Handbook of Free Radicals and Antioxidants in Biomedicine, Vol. 1, CRC Press, Boca Raton, 1989, p. 37.
[48] K.H. Fantes, I.G. Furminger, Nature 215 (1967) 750.
[49] W.M. Mitchell, Biochim. Biophys. Acta 147 (1967) 171.
[50] J.M. Brewer, Science 156 (1967) 256.
[51] E. Penton, Eur. Patent Publication No EP 480525 (1992).
[52] D. Tleugabulova, J. Chromatogr. B 713 (1998) 401.
[53] H. Esterbauer, G. Striegl, H. Puhl, M. Rotheneder, Free Radical Res. Comm. 6 (1989) 67.
[54] N.S. Pujar, A.L. Zydney, J. Chromatogr. A 796 (1998) 229.
[55] K. Dill, Biochemistry 29 (1990) 7133.
[56] H. Esterbauer, H. Zollner, J. Schaur, in: C. Pelfrey (Ed.), Membrane Lipid Oxidation, CRC Press, Boca Raton, 1990, p. 239.
[57] R.T. Dean, S. Fu, R. Stocker, M.J. Davies, Biochem. J. 324 (1997) 1.
[58] D. Tleugabulova, V. Falcón, E. Pentón, J. Chromatogr. B 720 (1998) 153.
[59] N.I. Nisevich, V.F. Uchaikin, T.P. Moleva, Pediatria (Russian) 6 (1978) 44.
[60] J.M. Jongerius, M. Wester, H.T.M. Cuypers, W.R. van Oostendorp, P.N. Lelie, C.L. van der Poel et al., Transfusion 38 (1998) 56.